Science of the Total Environment 933 (2024) 173052

Contents lists available at ScienceDirect

Science of the Total Environment

journal homepage: www.elsevier.com/locate/scitotenv

Climate of the Pyrenees: Extremes indices and long-term trends

José María Cuadrat [a], Roberto Serrano-Notivoli [a,*], Marc Prohom [b], Jordi Cunillera [b], Ernesto Tejedor [c], Miguel Ángel Saz [a], Martín de Luis [a], Alba Llabrés-Brustenga [d], Jean-Michel Soubeyroux [e]

[a] Dept. of Geography and Regional Planning, Environmental Sciences Institute (IUCA), University of Zaragoza, Zaragoza, Spain
[b] Meteorological Service of Catalonia, Barcelona, Catalonia, Spain
[c] National Museum of Natural Sciences, MNCN-CSIC, Madrid, Spain
[d] Barcelona Supercomputing Center, Barcelona, Catalonia, Spain
[e] Météo-France, Toulouse, France

HIGHLIGHTS

- Development of the first transboundary gridded climate dataset for the Pyrenees.
- A comprehensive reconstruction process enables the study of climate changes in both space and time.
- Significant warming trends were identified at both annual and seasonal levels across the Pyrenees.
- Significant precipitation negative trends were observed on southern and Mediterranean sides.

GRAPHICAL ABSTRACT

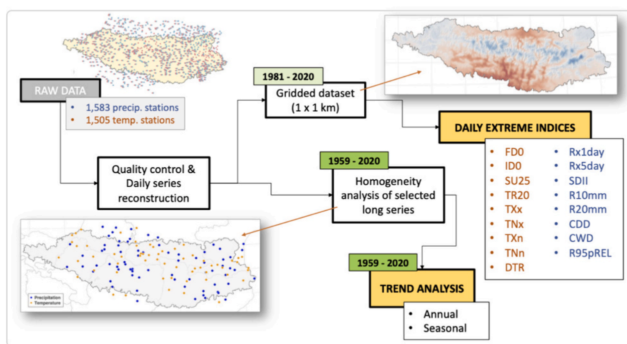

ARTICLE INFO

Editor: Paola Verlicchi

Keywords:
Mountain climatology
Precipitation
Temperature
Gridded dataset
Quality control
Homogenization

ABSTRACT

We utilized an extensive, multisource, cross-border dataset of daily meteorological observations from over 1500 stations in the Pyrenees, spanning from the mid-20th century to 2020, to examine the spatial and temporal climate patterns. Our focus was on 17 indices related to extreme precipitation and temperature events across the mountain range. The original data underwent rigorous quality control and homogenization processes, employing a comprehensive workflow that included spatial modeling based on environmental predictors. This process yielded two main outcomes: 1) a high-resolution gridded dataset (1 km^2) of daily precipitation, maximum and minimum temperature from 1981 to 2020, allowing for a detailed analysis of spatial variations; and 2) an evaluation of long-term annual and seasonal trends from 1959 to 2020, using selection of high-quality data series that were homogenized to preserve their temporal structure and coherence. The findings revealed a clear elevation-related pattern in temperature indices (with the exception of tropical nights, which were predominantly observed on the Mediterranean side) and a distinct north-south latitudinal disparity in precipitation, turning longitudinal when focusing on extreme precipitation events. Overall, there was a notable and significant warming trend of 0.2 to 0.4 °C per decade, and a non-significant change of precipitation, with the exception of

* Corresponding author.
E-mail address: roberto.serrano@unizar.es (R. Serrano-Notivoli).

https://doi.org/10.1016/j.scitotenv.2024.173052
Received 29 December 2023; Received in revised form 16 April 2024; Accepted 6 May 2024
Available online 10 May 2024

the southern and Mediterranean regions, where there was a notable decrease, approximately −3 % per decade, observed on an annual basis.

1. Introduction

Mountain areas are very sensitive to environmental variations, and they are among the most vulnerable regions to climate change and variability worldwide (Beniston et al., 1997; Giorgi et al., 1997; Pepin and Lundquist, 2008; El Kenawy et al., 2013; Wang et al., 2014). Nonetheless, the patterns of change are not uniform and display significant spatial and temporal disparities, necessitating further investigation to enhance our comprehension of long-term shifts and the regional-scale forces driving these changes. In recent years, many studies that focused on the behavior of the climate in the Pyrenean region have shown variations in the precipitation regime (e.g. López-Moreno et al., 2010; Buisán et al., 2015; Gascoin et al., 2015; Lemus-Canovas and López-Bustins, 2021), a progressive rise in temperatures, greater than the global warming (e.g. Bücher and Dessens, 1991; Spagnoli et al., 2002; Espejo et al., 2008; El Kenawy et al., 2011; Deaux et al., 2014) and an increase in the frequency of extreme events, becoming more evident in a lower snow cover and in the accelerated retreat of ice masses and glaciers (e.g. López-Moreno et al., 2008; Maris et al., 2009; Soubeyroux et al., 2011; Esteban et al., 2012; Pérez-Zanón et al., 2017; Serrano-Notivoli et al., 2018; OPCC-CTP, 2018; Lemus-Canovas and López-Bustins, 2021; Bonsoms et al., 2021; Albalat et al., 2022). Although these investigations used different spatial and temporal scales or diverse analytical approaches to evaluate the quality and homogeneity of the data, all of them showed an intensification of rainfall extremes and defined consistent and coherent patterns of warming, mainly since the second half of the 20th century, in line with the global diagnosis made by the latest report of the Intergovernmental Panel on Climate Change (IPCC, 2021). However, the analysis of climate in such complex terrain as the Pyrenees require more than the consideration of several locations with variable length of data series of observations. These data should be complemented with continuous spatial climatic information for which gridded datasets are fundamental. Previous research in other mountain areas showed the benefits of this type of products (e.g. Daly et al., 2017; Rubel et al., 2017; Isotta et al., 2014).

In many cases, these studies used a low density of observations or were based on data from different meteorological networks with significant changes between countries and types of measurement that were not always harmonized. As a result, the findings have largely been confined to particular regions of the Pyrenees, presenting inherent challenges, and underscoring the need for a more holistic perspective. These limitations are the result of the diversity of the mountain climate, together with the low density of observatories and, sometimes, the administrative complexity of the different countries, all of which makes it difficult to unify climate information in a single project. In this sense, the HISTALP projects on the Alps (Auer et al., 2007) and CARPATCLIM on the Carpathians (JCR, 2010; CARPATCLIM, 2013) are remarkable landmarks in mountain climate research in Europe. These projects were a successful effort to provide broad and uniform climate databases, allowing for a good approximation to the knowledge of the climate in their respective territories.

With the same purpose in the Pyrenees, the CLIMPY (https://opcc-ctp.org/es/climpy) and OPCC-ADAPYR (https://opcc-ctp.org/es/proyecto/opcc-adapyr) projects, coordinated by the Pyrenean Climate Change Observatory (OPCC, https://www.opcc-ctp.org/es), have made possible the evaluation of the climate of the entire mountain range with the generation of a record of complete, temporally and spatially homogeneous, daily data of the precipitation and air temperature and their corresponding metadata for the period 1981–2020. This is the first initiative to create a single database with observations from all the meteorological stations available in the three Pyrenean countries (Spain, France, and Andorra). Data was quality controlled, homogenized, and reconstructed using a common methodology, which was crucial to analyze the essential characteristics of the climate of the Pyrenees and, at the same time, represent the most important regional variations. For this purpose, our work considers a subset of descriptive indices recommended by the WMO-WRCP Expert Team on Sector-specific Climate Indices (ET-SCI) of the World Meteorological Organization (Klein Tank et al., 2009), which unify criteria research and facilitate comparison between different regions. The calculation of the indices was done directly from the temperature and precipitation database created. The data is provided daily in a 1 × 1 km grid format, enabling detailed analysis of spatial patterns and variations in climate conditions. An extended analysis over a selection of a high-quality data series contributed to the analysis of temporal evolution and trends for the 1959–2020 period. The data set covers >1300 measurements on any given day of the study period and is, probably, one of the densest in situ monitoring systems available for a mountain range of this extent. Furthermore, the quality of the database was reviewed by updating existing cross-national information and by adopting a quality control procedure that addresses common data coding errors and involved several semi-automatic checks, with the aim of reducing the risk of underestimations, especially at high altitudes.

This study aims to achieve two main goals: 1) to reveal the spatial patterns of extreme temperature and precipitation in the Pyrenees in recent decades, using 17 climate indices; and 2) to examine the temporal trends as indicators of climate variability and for monitoring climate change. The findings are displayed in maps for easier understanding, and the full database is accessible and available for free download online at https://zenodo.org/doi/10.5281/zenodo.3611126.

2. Methods

2.1. Study area

The Pyrenees form a natural border between France, Spain, and Andorra located in the northeastern part of the Iberian Peninsula. Stretching 450 km from west to east, this mountain range extends from the Atlantic Ocean to the Mediterranean Sea. In its central sector, it spans over 150 km in width, constituting a compact and massive mountain range on the peninsular isthmus. The Pyrenees dominate the geographical context with altitudes higher than 2500 m a.s.l. and numerous summits exceeding 3000 (e.g., Aneto, 3404; Posets, 3375; Monte Perdido, 3355; Vignemale, 3298; Balaitus, 3144), along with other forms of relief such as long depressions and a variety of intermediate valleys, which contribute to its notable topographic and landscape diversity. On both sides of the central alignment of the mountain range are the foothills of the pre-Pyrenees, formed by a set of mountain units of medium altitude and very different structure between the French and Spanish slopes: the northern slope is steeper than the southern slope, rarely exceeding 50 km in width, while the Spanish Pre-Pyrenees sometimes exceeds 100 km. Furthermore, the eastern area of the Pyrenees is wider than its western area, with notable mountain centers such as the great Corbières massif in the northeast and various mountain ranges in Catalonia.

The study area (Fig. 1), defined by the Working Community of the Pyrenees (CTP), involves the French regions of Aquitaine, Midi-Pyrénées and Languedoc-Roussillon; the Principality of Andorra; and the Spanish Autonomous Communities of Catalonia, Aragon, Navarre, and the Basque Country. The complete area spans 55,292 km^2 with 656 km of national administrative borders.

The Pyrenean region is located at the crossroads between three well-defined climatic zones: the Atlantic, the Mediterranean and the Continental areas. The Pyrenees are shaped by orographic effects, resulting in a diverse climatic mosaic across the mountain range. This leads to a stark contrast between the French and Spanish sides, which is clearly evident in the differences in vegetation and landscape. Temperatures progressively decrease with elevation, with annual averages exceeding 10 °C in the Pre-Pyrenees and below 4 °C on the highest peaks, where glaciers indicate tundra and perpetual ice climate types. Precipitation is spatially irregular and presents important variations depending on the altitude, exposure to humid winds, and the presence of orographic barriers of regional importance. The best exposed areas (Atlantic side) exceed 2000 mm per year, while the lands sheltered and at inner lower elevations barely reach 1000 mm. Furthermore, the Pyrenees are a compact group of high massifs compared to the surroundings, which produces a sharp increase in precipitation, defining islands of humidity that tend to reproduce the organization of the relief (Cuadrat et al., 2007).

2.2. Data

The original raw dataset included daily precipitation (PPT) and maximum (TX) and minimum (TN) temperature from three countries: Spain, France, and Andorra, and four agencies: Spanish Meteorological Agency (AEMET); MétéoFrance (MF), Meteorological Service of Catalonia (SMC) and National Meteorological Service of Andorra (SMNA). A total of 1505 temperature and 1583 precipitation stations comprised the complete database, encompassing the whole period 1959–2020. Nevertheless, since the temporal coverage is not homogeneous for the entire period (e.g., many French observatories have data from the late 1950 decade), two separated periods were considered: 1959–2020 for the analysis of long-term behavior, and 1981–2020, with a greater presence of weather stations, for the generation of a grid allowing a detailed analysis of changes in spatial patterns.

2.2.1. 1981–2020 period

Although the temporal period spanned the years from 1959 to 2020, the gridded dataset was constrained to 1981–2020 period, when the available number of stations and their spatial distribution properly covered the study area. After a first selection of those inside a radius of 50 km around the Pyrenees limits and within the shorter period, the station network resulted in 949 and 1202 observatories of temperature and precipitation, respectively.

The temporal availability varied from approximately 200 to 400 stations/year for temperature and from 400 to 650 for precipitation (Fig. 2a). However, there was a higher internal variability (higher differences of available stations between days within a year) from the mid-2010 decade, when the number of data increases. While the data adequately spanned the spatial domain, a majority of the stations were situated in lowland areas. Only 6.9 % of the total stations were located above 1500 m above sea level (m a.s.l.), leading to an underrepresentation of the observed climate in the Pyrenean region. This is notable considering that areas higher than this elevation threshold constitute 17.8 % of the region. Most of the stations were located in towns within valleys, especially in earlier periods, making it challenging to obtain long-term data series from highlands areas.

The average missing data per station varied by decades from 38.5 to 51.8 % in precipitation and from 39.6 to 64.3 in temperature (Table 1). However, the high standard deviation in all cases (around 40 %) indicated that the number of missing data was very different between stations.

2.2.2. 1959–2020 period

In order to assess long-term trends, sufficiently long time series are needed and preferably with few gaps. Unfortunately, in the initial database, the number of observatories with continuous data and no location changes since 1959 was anecdotal. For example, the average length of temperature series associated with a single observatory was 21 years, and only 25 % of them covered >50 years. For this reason, to obtain long enough series and grasp the long-term trend and variability, we proceeded to the composition or merging of series according to some minimum criteria established by previous studies (Klein Tank et al., 2009; Squintu et al., 2020). In the case of temperature, the following criteria was established: (1) a maximum distance of 20 km, (2) a difference in altitude of <50 m, (3) location within the same geographical unit (valley, basin, plateau) and (4) a maximum of three series sections to obtain a single series. In the case of precipitation, the minimum distance was set at 10 km, and the difference in altitude 25 m.

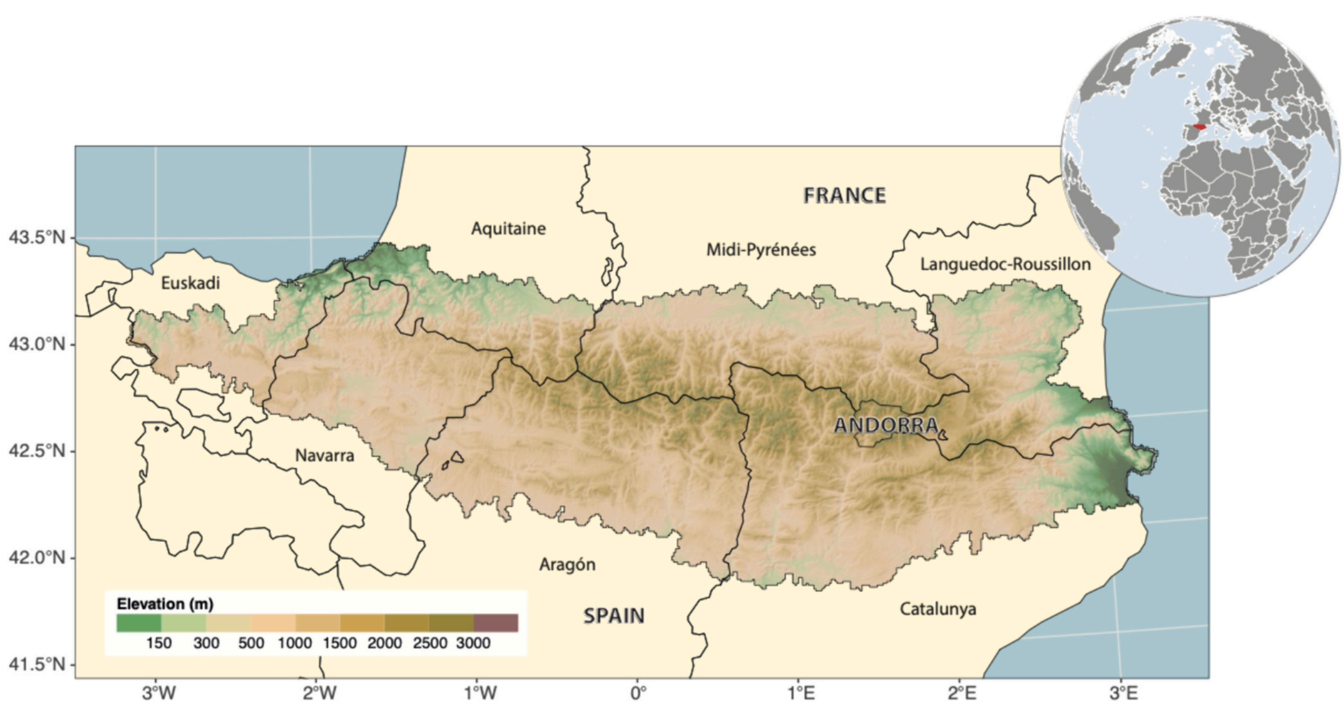

Fig. 1. Pyrenees spatial domain (shaded area with topography) and administrative regions.

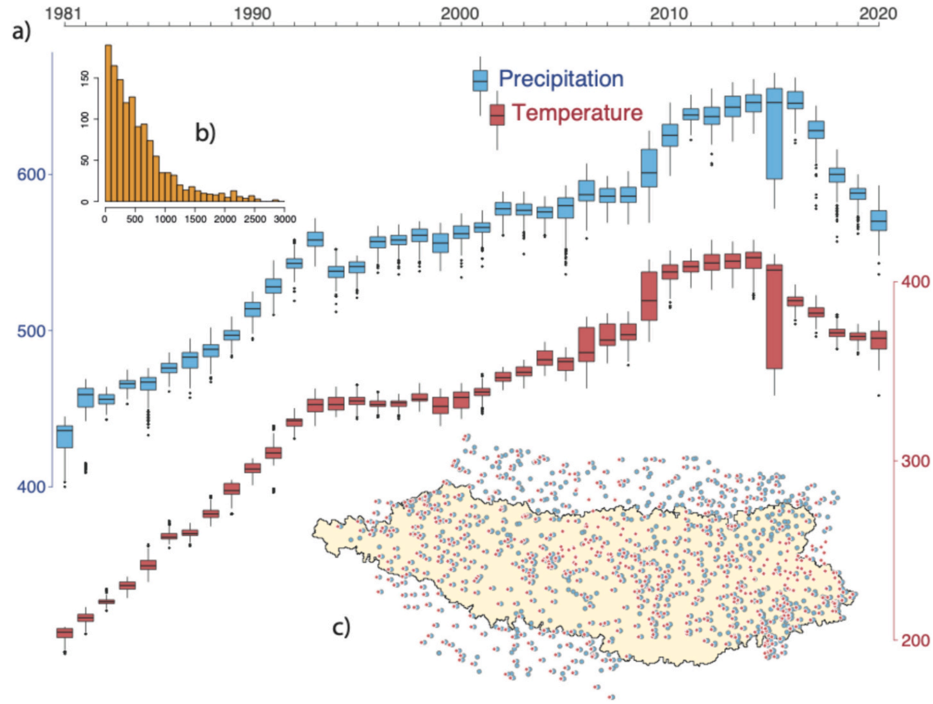

Fig. 2. a) Annual availability of daily precipitation (blue boxplots) and temperature (red boxplots) data. b) Histogram of stations' distribution by elevation ranges. c) Location of precipitation (blue dots) and temperature (red dots) stations.

Table 1
Mean number of stations (n) and missing data (MD, %) (and standard deviation between brackets) by decades and the complete period.

		1981–1990	1991–2000	2001–2010	2011–2020	1981–2020
Precip.	n	766	845	900	888	1202
	MD	51.8 (44.6)	44.1 (43.9)	40.9 (43.9)	38.5 (42.1)	43.9 (32.9)
Temp.	n	503	616	699	695	949
	MD	64.3 (42.1)	52.2 (44.0)	46.5 (43.4)	39.6 (43.1)	50.7 (30.6)

As a result, a total of 61 temperature (TX and TN) and 119 precipitation series covering the period 1959–2020 were compiled. Fig. 3 shows the location of the series according to the variable observed. Section 3.3 describes the quality control and homogeneity analysis applied.

2.2.3. Climate indices calculation

Lastly, 9 temperature-based and 8 precipitation-based indices were calculated following Klein Tank et al. (2009) over the gridded dataset and at the selected long-term stations (Table 2).

2.3. Quality control, series reconstruction and gridding

Modeling precipitation in complex terrain is a real challenge since not only great variations on short spatial scales can be produced but also the availability of observations is not the same as in lowlands. The procedure of precipitation reconstruction, which is fully described in Serrano-Notivoli et al. (2017a, 2017b) involves the selection of nearest stations for each grid point, and the modeling of a new estimate based on their observations and their environmental metadata (longitude, latitude, elevation, and distance to the coast). These covariates perform the

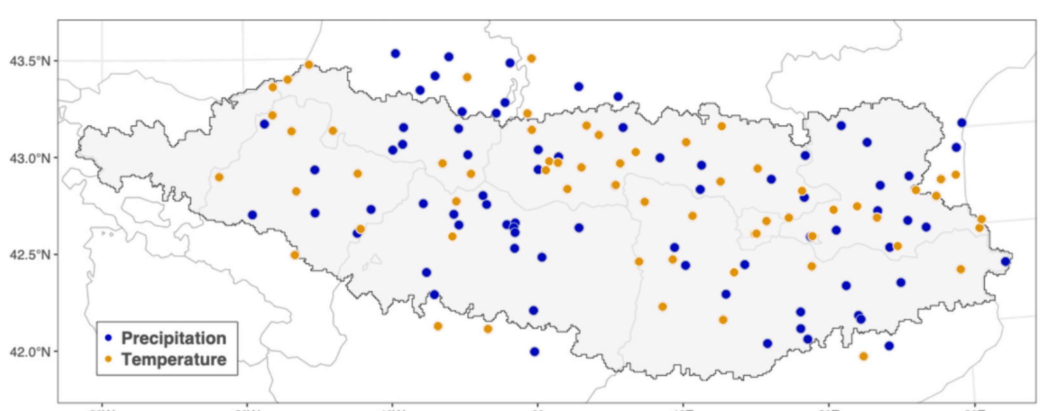

Fig. 3. Location of temperature and precipitation series covering the period 1959–2020.

Table 2
Definition of the 17 indices calculated over the daily gridded dataset and selected series.

Acronym	Description	Units
Temperature		
FD0	Number of frost days: annual count of days when TN < 0 °C	Days
SU25	Number of summer days: annual count of days when TX > 25 °C	Days
ID0	Number of icing days: annual count of days when TX < 0 °C	Days
TR20	Number of tropical nights: annual count of days when TN > 20 °C	Days
TXx	Monthly maximum value of TN	°C
TNx	Monthly maximum value of TN	°C
TXn	Monthly minimum value of TX	°C
TNn	Monthly minimum value of TX	°C
DTR	Daily temperature range: monthly mean difference between TX and TN	°C
Precipitation		
Rx1day	Monthly maximum 1-day precipitation	mm
Rx5day	Monthly maximum consecutive 5-day precipitation	mm
SDII	Simple precipitation intensity index: average precipitation in wet days (PPT ≥ 1 mm)	mm
R10mm	Annual count of days when PPT ≥ 10 mm	Days
R20mm	Annual count of days when PPT ≥ 20 mm	Days
CDD	Maximum length of dry spell, maximum number of consecutive days with PPT < 1 mm	Days
CWD	Maximum length of wet spell, maximum number of consecutive days with PPT ≥ 1 mm	Days
R95pREL	Relative contribution of RR > 95th percentile to annual total PPT	%

influence of the boundary effect (latitude), differences in altitude gradients (elevation), etc., in the modeling of each individual grid point at each different day.

The methodological process until the grid creation was developed in three steps: 1) implementation of a comprehensive quality control to the observations, flagging suspect records according to predefined climate-based criteria; 2) reconstruction of serially complete time series by estimating new values to missing observations in the original dataset; and 3) creation of new time series at every grid point based on the reconstructed data series with >10 years of observations.

The quality control process (QC) was based on the comparison of observations (*Obs*) with their corresponding reference values (RVs), which are estimates calculated with a Generalized Regression Model (GLM), where nearest observations (*NObs*) act as the dependent variable and environmental metadata act as predictors. In the case of precipitation, RV results from two estimates: i) a binomial prediction of the probability of occurrence of a wet day; and (if there is a significant probability of rain) ii) an estimate of the amount of precipitation. The QC runs in an iterative mode. For precipitation, five criteria are applied until no suspect values are detected: 1) suspect rain: $Obs > 0$ & $Nobs = 0$; 2) suspect zero: $Obs = 0$ & $Nobs > 0$; 3) suspect outlier: $Obs \geq 10RV$ | $Obs \leq 10RV$; 4) suspect dry: $Obs = 0$ & $p(wet\ day) > 0.99$ & $RV > 5$; and 5) suspect wet: $Obs > 5$ & $p(dry\ day) > 0.99$ & $RV < 0.1$. For temperature, an initial basic QC (internal coherence, impossible values, duplicated values) was followed by a progressive comparison of *Obs* and *RV* at monthly and daily scale running tests to check: i) correlation analysis; ii) spatial anomalies; iii) temporal anomalies; and iv) spatio-temporal anomalies. The QC process is detailed in Serrano-Notivoli et al. (2017a, 2019).

After QC, the daily series reconstruction consisted of calculating new RVs based on the cleaned dataset that were used to replace the missing values in the original series, producing a serially complete dataset. The advantage of this process is that all of the available data can be used as there are no restrictions imposed due to the length or structural characteristics of the series.

Using the same procedure based on the calculation of RV, new estimates were computed to build a 1 × 1 km spatial resolution grid of daily precipitation, maximum and minimum temperature. For each point of the grid and each day of the total period, RVs were computed based on the data of the 10 *NObs* for precipitation and the 15 *Nobs* for temperature.

2.4. Long-term homogenization

Homogenization of time series is required specially for those data series that are long enough to be used in climate trend and climate variability analysis. The main objective of homogenization is to detect and remove the effects of non-climatic factors in a climate series, which can be grouped into (1) changes in the conditions in which the observations are taken (i.e. type of weather station, relocation, instrumentation, observation methods, etc.) and (2) changes in the immediate environment surrounding the weather station (urbanization is the most common). It is clearly demonstrated that homogenized data characterize the true climatic variations better than raw climate observations (Venema et al., 2020; Aguilar et al., 2003).

In this study, the ACMANT method (Applied Caussinus-Mestre Algorithm for the homogenization of Networks of climate Time series) was used. ACMANT is a relative homogenization method (i.e. it is based on the temporal-spatial comparison of observed data), and it was developed during the European project COST ES0601 ("HOME"; Venema et al., 2012), It has been recognized as one of the most efficient tools for detecting inhomogeneities in climate series (Domonkos et al., 2021; Guijarro et al., 2017). Version 4 of ACMANT was used to homogenize the daily Pyrenean series (TX, TN and PPT) and is based on an automatic procedure that includes a basic quality control of data (physical outliers) and several iterations to detect all potential inhomogeneities (see Domonkos, 2022 for more details). At the end, a complete list of breakpoints is released for each climate series, jointly with the adjustment applied (based on an ANOVA correction model). In addition, the method includes infilling of data gaps.

Some statistics resulting from the homogenization are shown in Table 3. Temperature series revealed a large number of breakpoints compared to precipitation, as a consequence of the greater temporal and spatial variability of this last variable, that makes more difficult the detection of inhomogeneities. Nevertheless, as is shown in Fig. 4, in most cases, the adjustment or size of the breaks were restricted within the −1 or 1 °C range (for example, in the case of the TX, this range accounted for 74 % of the total adjustments applied). For precipitation, the multiplicative adjustment in most of the series (54 %) was in the range of 0.85 and 1.15.

2.5. Trends

Trend analysis is applied to datasets by minimizing square errors of linear trends, and it is made using the Mann-Kendall trend test (Mann, 1945; Kendall, 1975). This non-parametric test is commonly used to detect trends in long time series datasets, and it was used before by the authors to detect temperature and precipitation trends at the study area in previous works (Cuadrat et al., 2013; Prohom et al., 2023). Trends are considered statistically significant when the *p*-value is equal to or <0.05, and they are always referred as decadal change (°C/decade for temperature or %/decade for precipitation).

Table 3
Long-term series (1959–2020) homogenization statistics from ACMANTv4.

	TX	TN	PPT
Number of time series	61	61	119
Average number of break points per data series	4.9	5.2	1.2
Maximum number of breakpoints in a single series	11	9	5
Number of series with <3 breakpoints in TX and TN, and <1 in PPT	17 (28 %)	12 (20 %)	74 (62 %)

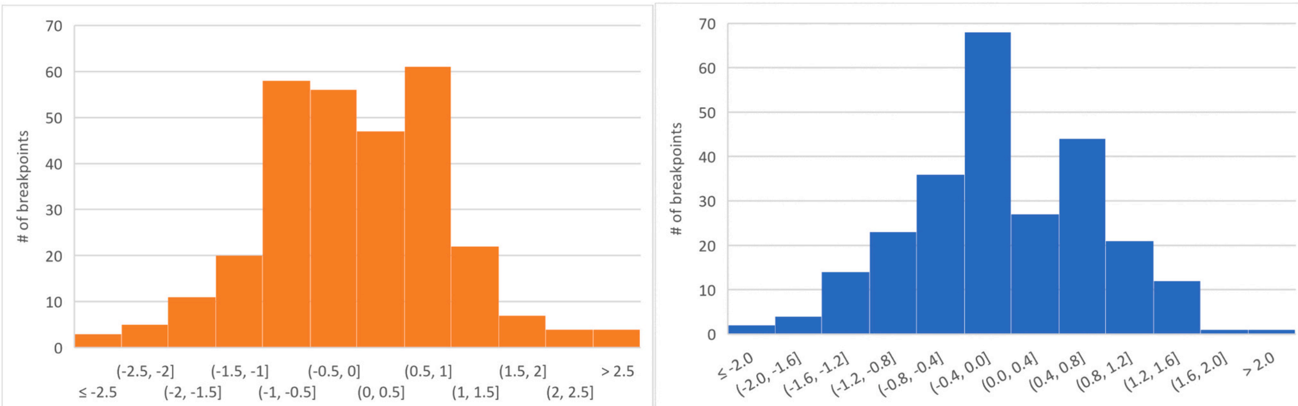

Fig. 4. Histograms with the distribution of the size of the breakpoints for TX series (left) and TN series (right).

3. Results

3.1. Temperature

Temperature indices are the expression of both the effect of altitude and the influence of different types of climates, in addition to showing the differences between the northern and southern slopes of the mountain range. Two gradients are common to all spatial distributions: i) the progressive decrease in altitude towards the French and Spanish Pre-Pyrenees explains the gradient of temperature in the same direction, from the high peaks to the northern and southern lowlands; and ii) from the central Pyrenees in westward and easterly directions as a consequence of the progressive increase of Atlantic influence or the greater presence of Mediterranean dominance. A clear example of these gradients is the spatial pattern of the daily thermal oscillation (DTR) (Fig. 5): in the high altitudes of the central Pyrenees the average monthly difference between the maximum temperature and the minimum temperature is low, <6 °C; but this value increases rapidly with the altitudinal decrease until it widely exceeds 12 °C in the central valleys of Aragon and Catalonia, which indicates an evident effect of continentality that stands out compared to the more moderate values of the regions close to the Atlantic Ocean and the Mediterranean Sea.

This general scheme is repeated when examining the averages of the maximum and minimum values of the maximum and minimum temperatures (TXx, TNx, TXn, TNn) (Fig. 6). In all cases, the elevation gradient clearly identifies the highest areas of the mountain range and the sectors most protected from maritime influence. Although the spatial variation of the variables is quite gradual and uniform, greater changes are observed in the maximum temperatures, whose values indicate notable differences between them, especially between the main axis of the mountain range and the vicinity of the Catalan coast.

The dependence on orography is particularly visible when counting days with cold and warm temperatures. The average annual number of frost days (FD0) varies from <30 at low altitudes near the sea to >180 days at altitudes above 2000 m (Fig. 7). Between these extremes there is a clear gradient that highlights the continental conditions of the headwaters of the interior valleys of Midi-Pyrénées, Aragon and Catalonia compared to the thermal softness that is observed towards both limits of the mountain range in contact with the maritime influence. Logically, this distribution coincides with the map of the number of days with ice (ID0) whose amount is >10 days in a wide sector of the central Pyrenees but decreases towards the Atlantic and Mediterranean coast until reaching averages that barely add up to one day. In contrast, the occurrence of summer days (SU25), with temperatures above 25 °C, is almost non-existent at the higher peaks. However, the Pyrenees are not free from hot days. The valleys in the central Spanish Pyrenees and areas closer to the Mediterranean frequently exceed 100 such days annually, in stark contrast to the milder temperatures observed on the French and Western sides. This difference once again highlights the distinct climatic variations between the Atlantic and Mediterranean regions. However, when considering tropical nights (TR20), where minimum temperatures exceed 20 °C, the thermal pattern is more uniform. Only a small portion of the eastern sector of the mountain range experiences >10 tropical nights per year. In the rest of the region, due to the altitude, it is rare for minimum temperatures to surpass 20 °C.

The central Pyrenees, which extends across Aquitaine, Midi-Pyrénées, Andorra, Aragón, and Catalonia, is probably the most relevant region for observing some of the key characteristics of air temperature in the Pyrenees. The spatial pattern of most of the estimated indices (DTR, TXx, TNx, TXn, TNn, FD, ID) shows exceptional values that are not recorded in the rest of the mountain range. The succession and duration of cold moments, periods with ice or minimum temperatures are a fundamental part of the climate of this region.

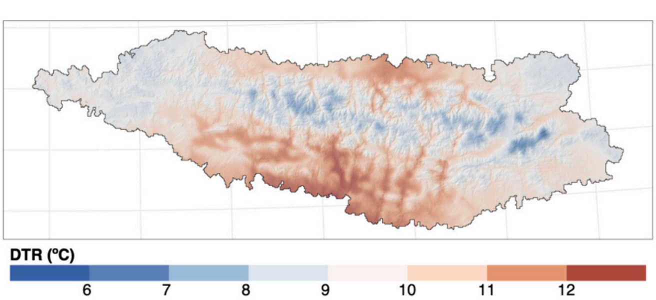

Fig. 5. Average (1981–2020) diurnal temperature range (DTR).

3.2. Precipitation

In the case of precipitation, the indices also show the different influences conditioning the climate of the mountain range, but the most outstanding facts are the marked contrasts between the Atlantic and Mediterranean slopes, and also between the French Pyrenees and the Spanish Pyrenees, which are closely related to the dominance of the oceanic climate and exposure to humid westerly wind flows. The succession and duration of the periods of consecutive wet and dry days (threshold of 1 mm) confirms this dipole and highlight one of the fundamental characteristics of the Pyrenean rainfall (Fig. 8). Throughout the Atlantic sector, the length of wet spells (CWD) exceeds 16 days per year and remains at high values in the north of Navarra, Aquitaine, and part of Midi-Pyrénées. From here, the frequency drops by almost a third towards Aragón, Catalonia and the Mediterranean coast, where the average in some areas can be <6 days. For the dry spells, the asymmetry is reversed, and the length of the dry periods (CDD) barely reaches 15 days on the French and northern slopes of Navarra, while they increase towards the Mediterranean coast and, in particular,

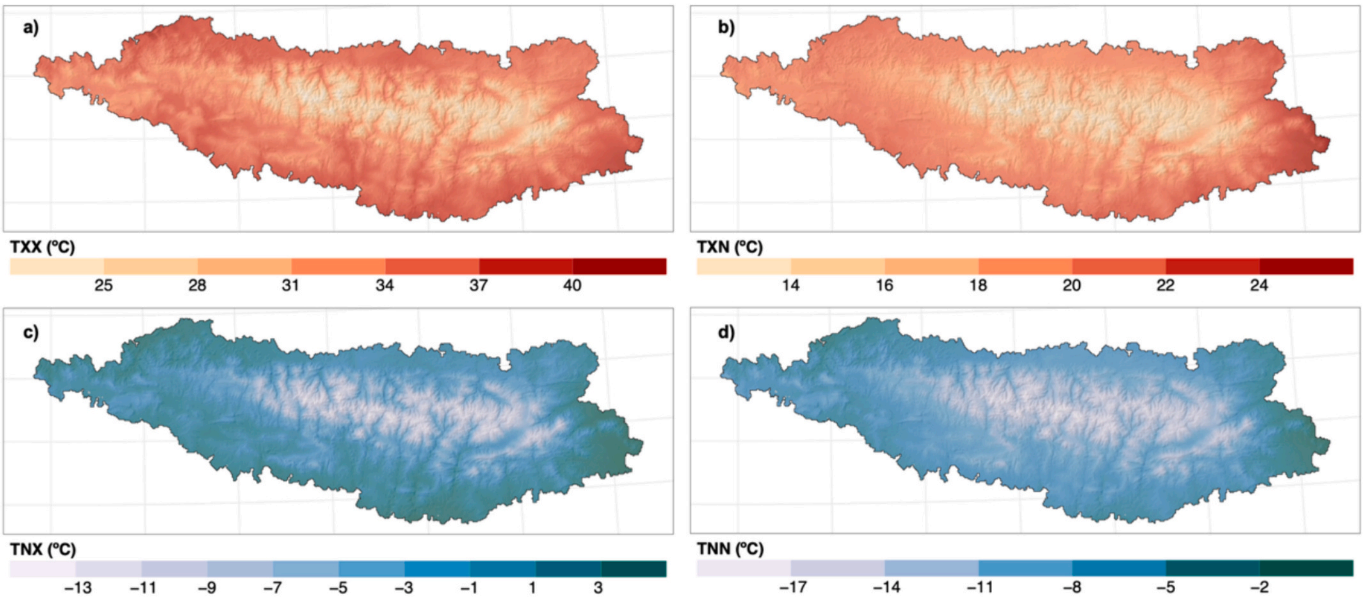

Fig. 6. Average (1981–2020) extreme temperature indices: a) TXX; b) TXN; c) TNX; d) TNN.

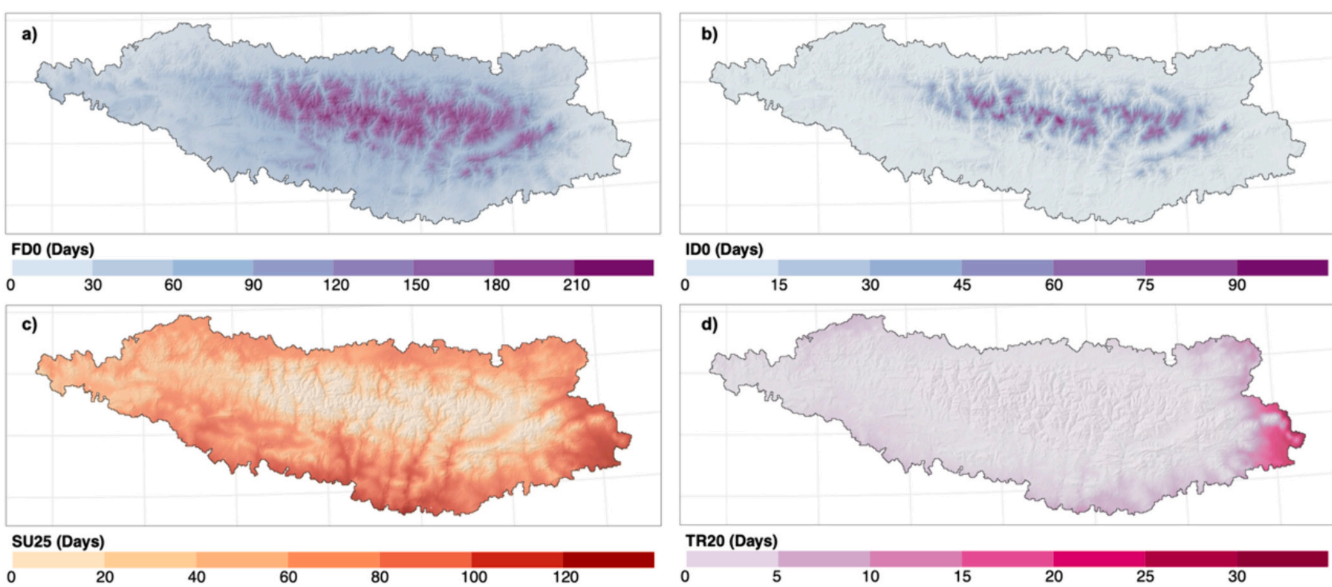

Fig. 7. Average (1981–2020) extreme temperature indices: a) FD0; b) ID0; c) SU25; d) TR20.

towards the sheltered areas of the Pre-Pyrenees of Aragon and Catalonia where particularly long streaks of dry days are recorded, the average duration of which can exceed 40 days.

The different indices, but in particular the daily precipitation intensity index (SDII), reveal that the central regions of the Pyrenees seem to be well protected from rainy weather systems by the surrounding relief and, consequently, precipitation is less frequent, however, they can be affected by very intense rains. In the Catalan Pyrenees and, especially in the Aragonese, average daily values of >16 mm are reached (5.3 % of all territory), and in several points, they exceed 20 mm (0.6), which indicates the presence in these regions of very intense rainy episodes, favored by the orographic effect, despite being far from the marine masses. At both ends of the mountain range the intensity increases, favored by the Atlantic storms and the Mediterranean depressions, in each case, but to a more limited extent. This spatial scheme is partially repeated with the selected indices of maximum precipitation in one day (Rx1day) and five days (Rx5day), in which the high concentration of the highest values in areas close to the Atlantic and the Mediterranean is evident (Fig. 9). Such is the case of specific areas of the central Pyrenees where, on average and above 1800 m, values >200 mm were recorded in 24 h over the course of a year. These results are clear exponents of the strong territorial contrasts that exist in the Pyrenees, and at the same time indicate the diversity and rainfall complexity of the Pyrenean Mountain range.

Precipitation >10 mm in 24 h (R10mm) is frequent throughout the Pyrenean mountain range, but with important territorial nuances: again, in the regions with clear Atlantic influence the rainfall exceeds this amount for a good number of days a year, more 80 days in some environments privileged by the orography and exposure; On the other hand, the values decrease rapidly towards the south and east of the mountain range, where the annual average in some sectors can be <20 days. When the days in which precipitation is >20 mm (R20mm index) are counted, the magnitude range is much lower, but the spatial distribution of this index is very similar to that of R10mm. Also, very rainy events in which

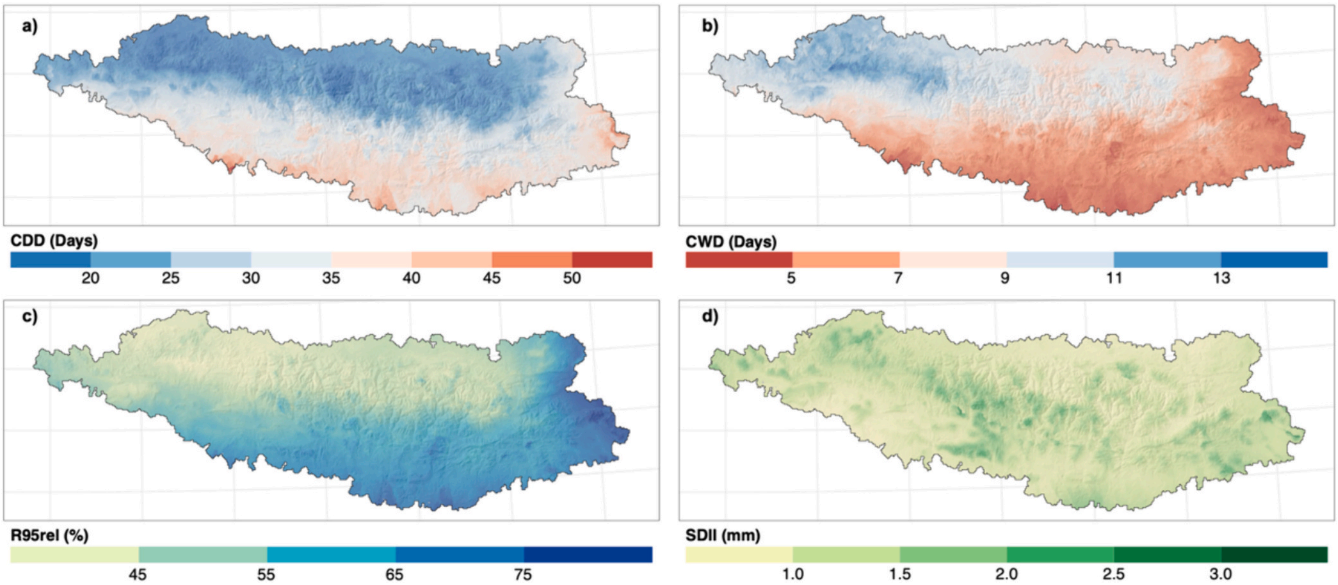

Fig. 8. Average (1981–2020) extreme precipitation indices: a) CDD; b) CWD; c) R95rel; d) SDII.

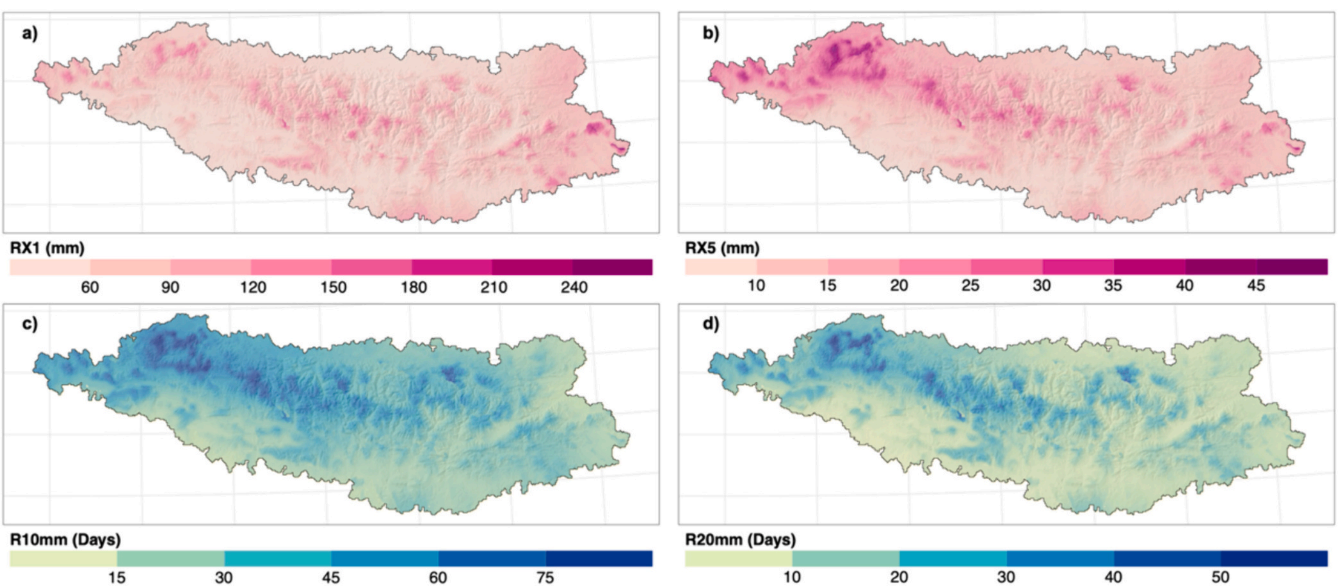

Fig. 9. Average (1981–2020) extreme precipitation indices: a) RX1; b) RX5; c) R10mm; d) R20mm.

daily precipitation has exceeded the 95th and 99th percentiles show concentration of the highest levels of extreme precipitation in elevated areas of the central Pyrenees and towards the Atlantic coast, where there is a 5 % probability that it will occur, exceed 500 mm; while these quantities experience a gradual decrease towards Languedoc-Rousillon and Catalonia, and as we descend in altitude, they rarely exceed 200 mm.

3.3. Long-term trends

Table 4 shows annual/seasonal trend values for mean, maximum and minimum temperature series (TM, TX and TN, respectively) at the Pyrenees and for the mentioned period 1959–2020. All positive trend values (except for TN in winter) are statistically significant according to the established condition (p-value ≤ 0.05), so behavior of this variable during the last 62 years at the Pyrenees is very clear. Annual mean temperature (TM) has increased +0.26 °C/decade in the whole mountain range, and the increase is greater for annual maximum

Table 4
Annual and seasonal trend values (°C/decade) for mean (TM), maximum (TX) and minimum (TN) temperatures at the Pyrenees for the period 1959–2020. Values in **bold** are statistically significant (p-val < 0.05) and values in *italics* are not significant. Values between brackets are the 95 % confidence interval.

	TM	TX	TN
Annual	**+0.26** [0.19, 0.33]	**+0.31** [0.22, 0.39]	**+0.21** [0.15, 0.27]
Winter (DJF)	**+0.17** [0.02, 0.33]	**+0.23** [0.05, 0.40]	*+0.12* [−0.03, 0.26]
Spring (MAM)	**+0.29** [0.17, 0.41]	**+0.35** [0.20, 0.51]	**+0.23** [0.13, 0.32]
Summer (JJA)	**+0.38** [0.27, 0.48]	**+0.43** [0.29, 0.57]	**+0.32** [0.24, 0.40]
Autumn (SON)	**+0.21** [0.09, 0.33]	**+0.23** [0.09, 0.38]	**+0.18** [0.08, 0.29]

temperature (TX, +0.31 °C/decade) than for annual minimum temperature (TN, +0.21 °C/decade). Seasonally, TM, TX and TN trend values are positive (increase), but greater values are obtained especially in summer (June, July and August) and also in spring (March, April and May). Moreover, the increase of temperature is very similar in all the study area, with practically no difference between Northern and Southern slopes or between Atlantic and Mediterranean slopes (annual TM trend value in these four areas is +0.26 °C/decade, annual TX trend values vary between +0.30 °C/decade and +0.32 °C/decade, and annual TN between +0.21 °C/decade and +0.22 °C/decade).

Table 5 shows annual/seasonal trend value for accumulated precipitation series (PPT) during the period 1959–2020 for the whole Pyrenees, and for four subregions of this range: Northern Pyrenees (similar to French Pyrenees), Southern Pyrenees (Spanish Pyrenees and Andorra), Atlantic Pyrenees (approximately the western half of the range, Atlantic influence) and Mediterranean Pyrenees (approximately the eastern half of the range, Mediterranean influence). Contrary to the temperature, in general precipitation trend values are not statistically significant, so it is difficult to come to a robust conclusion about the evolution of precipitation during the last six decades in the Pyrenees. The annual precipitation trend in the region shows a negative trajectory, decreasing by −1.4 % per decade (or −8.8 % over the last 62 years). However, as previously mentioned, this trend is not statistically significant. Another difference with temperature is that precipitation shows a different evolution pattern in the four studied regions of the Pyrenees. Although only two trend values show a p-value equal to or <0.05 (annual PPT in Southern Pyrenees, −2.8 %/decade, and annual PPT in the Mediterranean Pyrenees, −2.9 %/decade), decrease in the annual precipitation is greater in these two areas (Southern and Mediterranean Pyrenees), and especially due to a decrease in winter and summer precipitation. The precipitation trend values for the Atlantic and Northern Pyrenees are, in general, close to zero, so changes in accumulated precipitation are not significant.

Extreme climate indices trends (see Tables S1 and S2) confirmed this general decreasing precipitation behavior. For instance, the average precipitation per rainy day (SDII) resulted in a negative (significant) trend (−0.16 (mm/day)/decade), being higher in Southern and Mediterranean Pyrenees (−0.24 and −0.21 (mm/day)/decade, respectively) than in Northern and Atlantic areas (−0.07 and −0.12 (mm/day)/decade, respectively). The annual number of rainy days did not show a significant trend in the mountain range as a whole (average trend: −0.48 days/decade), but it was negative in Southern, Mediterranean and Atlantic Pyrenees (−1.25, −1.17 and −0.11 days/decade, respectively) and positive in Northern area (+0.38 days/decade). Lastly, the annual total precipitation in wet days (PRCPTOT) showed a negative trend in all Pyrenean areas (mean trend value: −16.50 mm/decade), being significant in Southern and Mediterranean areas (−29.51 and −26.72 mm/decade). These trend values indicated a major and clearer decrease of precipitation in Southern and Mediterranean Pyrenees than in Northern and Atlantic areas.

Table 5
Annual and seasonal trend values (%/decade) for accumulated precipitation for the period 1959–2020 at the Pyrenees and four areas of this mountain range. Values in **bold** are statistically significant and values in *italics* are not statistically significant. Values between brackets are the 95 % confidence interval.

	Pyrenees	Northern Pyrenees	Southern Pyrenees	Atlantic Pyrenees	Mediterranean Pyrenees
Annual	*−1.4* [−3.3, 0.5]	*−0.2* [−2.2, 1.9]	**−2.8** [−5.0, −0.7]	*−0.8* [−2.7, 1.1]	**−2.9** [−5.2, −0.5]
Winter (DJF)	*−2.3* [−7.2, 2.6]	*−1.0* [−5.6, 3.7]	*−4.1* [−10.3, 2.2]	*−1.6* [−6.7, 3.4]	*−4.2* [−10.1, 1.7]
Spring (MAM)	*−0.2* [−3.3, 2.9]	*+0.7* [−2.5, 3.8]	*−1.2* [−4.8, 2.5]	*+0.1* [−3.2, 3.3]	*−0.9* [−4.5, 2.8]
Summer (JJA)	*−2.1* [−6.2, 2.0]	*−0.4* [−4.8, 3.9]	*−3.8* [−8.1, 0.6]	*−0.9* [−5.5, 3.7]	*−3.8* [−8.1, 0.4]
Autumn (SON)	*−2.0* [−5.9, 1.9]	*−0.7* [−4.7, 3.3]	*−3.3* [−7.7, 1.1]	*−1.8* [−6.1, 2.5]	*−2.5* [−6.7, 1.6]

Regarding compound indices (see Fig. S2), winter cold/dry (CD) day trend values were positive in all the analyzed Pyrenean areas and statistically significant in Southern and Mediterranean Pyrenees (0.68 and 0.66 days/decade, respectively). Cold/wet (CW) days trend values were negative in all areas and statistically significant in Mediterranean Pyrenees (−0.23 days/decade). These results suggested a general decrease of snow cover, especially in Southern and Mediterranean Pyrenees, as shown in previous research (e.g. López-Moreno et al., 2020). On the other hand, summer warm/wet (WW) day trend values were close to zero in all studied areas, while warm/dry (WD) day trend values were positive (increase) and statistically significant in all areas, due to a clear increase of summer temperatures and a decrease of summer precipitation.

4. Discussion

The climate indices formulated by the ETCCDI are important indicators of the state of the climate. They are valid on a global, regional, and local scale, easy to understand and at the same time have a clear physical meaning (Williams and Eggieston, 2017). However, for these indices to provide reliable information, they must be supported by daily databases of high quality, in addition to having broad temporal coverage and high spatial resolution. Following this criterion, this work incorporates two important novelties with regard to high-resolution climate analysis in the Pyrenees: (i) a quality-controlled daily climate dataset in a high-resolution gridded of 1 × 1 km, and (ii) the calculation of a set of climate indices, focused mainly on extremes, covering a wide range of daily statistics and representing the most important regional variations. On the other hand, with regard to long-term analysis, this work provides (i) a unique daily database for temperature and precipitation in the Pyrenees for the period 1959–2020 and (ii) a subset of high quality and homogenized (using ACMANT method) series to study the temporal evolution of variables and their trends, both for the whole Pyrenees and for different subregions of this mountain range.

One of the most notable keys of the approach presented here is the use of all available climate information, which is crucial for a high-resolution result due to the observation network density having a major influence on gridded dataset results, controlling the skill of the final estimate of the variable (Merino et al., 2021; Hofstra et al., 2008). This is especially true at high percentiles, and therefore, at extreme indices (Hofstra et al., 2010). The results show that the method is capable of reproducing realistic climate situations; and at the same time, the comprehensive quality control detects a series of suspicious data in line with previous research (Serrano-Notivoli et al., 2017a, 2019), ensuring the elimination of anomalies in a spatial and temporal dimension.

In general, the results obtained agree with previous studies. In the case of thermal indices, their different intensity ranges have shown the strong dependence on altitude and greater or lesser proximity to the Atlantic Ocean and the Mediterranean Sea, recognized in recent Pyrenean works such as those carried out by Lemus-Canovas et al. (2021) or Pérez-Zanón et al. (2017), which were supported by high temporal and spatial resolution databases. What has already been pointed out at a lower resolution in the research by Lemus-Canovas et al. (2019) on the Pyrenees and by Esteban et al. (2012) is also confirmed and detailed in Andorra, or the more general approaches of Navarro-Serrano et al. (2018). Overall, results agree with Serrano-Notivoli et al. (2019), who identified similar spatial patterns to those obtained in our study over the Pyrenean area. Considering long-term (1959–2020) daily series of temperature (TX and TN) created in this work, annual and seasonal trend values also agree with previous studies (Esteban et al., 2012; Deaux et al., 2014; Pérez-Zanón et al., 2017); temperature has clearly increased during the last 62 years, especially since the mid 1980s decade (Fig. S1) (almost all trend values for TX and TN are statistically significant, with p-value much <0.05) and this behavior is very homogeneous in all Pyrenean areas. With respect to precipitation, as occurs in the main European mountain systems (e.g. Nigrelli and Chiarle, 2023; Cheval et al., 2014), its spatial distribution is more complex than that of temperatures due to its relationship with orographic roughness, and with exposure to moisture-carrying winds. However, most of the indices show a clear differentiated behavior between the French Pyrenees and the Spanish Pyrenees, in addition to the evident asymmetry between the Atlantic and Mediterranean slopes. This different behavior depending on the Pyrenean area or slope also appears in trend analysis of long-term (1959–2020) daily precipitation series, where decrease of annual precipitation is statistically significant for Southern Pyrenees and Mediterranean Pyrenees, but considering Northern or Atlantic Pyrenees the annual precipitation trend is close to zero. This complex and spatially variable pattern of precipitation is consistent with the results of previous work by Buisán et al. (2016), Lemus-Canovas et al. (2019) and Lemus-Canovas et al. (2021), in which the Pyrenean rainfall is related to the factors that condition it, such as: the Atlantic depressions, the main source of humidity, which can provide precipitation for several days to the best exposed areas; the influence of northern component advections, which retain precipitation on the French slope; and the occurrence of southern flow conditions, whose stagnation reinforces the intensity of precipitation in the high Pyrenean valleys. To which are added the Mediterranean depressions, responsible for episodes of notable intensity rain in the eastern Pyrenees, which provide high amounts of precipitation and cause strong contrasts in the daily records (Martin-Vide, 2004; Lana et al., 2009).

It's important to note that while the climate data grid utilized for calculating the indices covers the entire territory comprehensively, the original observations used to construct this grid are less frequent above 1500 m and become even rarer above 2000 m. This can cause, together with a non-measurable frequency of occurrence of thermal inversions in many valleys and humidity islands, that the relationships between the indices and the relief at high altitudes have more uncertainty. However, our results represent an important approximation to the extreme thermal and rainfall characteristics of the Pyrenees in the recent decades. The database created offers a valuable resource of information on the climate of the Pyrenean region. Indeed, the findings from this study have provided new insights on the distribution of mesoscale daily precipitation and temperature indicators, insights that would have been challenging to identify without a consistent cross-national data source. The dataset is also presented as a foundational resource for various applications including the assessment of regional climate models, serving as input for quantitative models of environmental subsystems, or enabling more accurate analysis of climate changes in mountain regions, which are particularly impacted by climate change.

5. Conclusions

We presented the first transboundary gridded climatic dataset of the Pyrenees in which meteorological data from Spain, France and Andorra were collectively analyzed. A comprehensive quality control of daily observations resulted in a filtered dataset that was divided in two periods:

i) 1981–2020: a 1 × 1 km spatial resolution gridded dataset of daily precipitation, maximum and minimum temperature was developed through spatial modeling using environmental predictors (elevation, longitude, and latitude). A collection of 17 climate change-related indices were calculated to account for spatial variations on annual averaged extreme precipitation and temperatures.
ii) 1959–2020: a curated collection of the longest and highest-quality data series formed the basis of the long-term dataset. Following a homogenization process to eliminate non-natural temporal climate variations, this dataset was utilized to calculate annual and seasonal trends in precipitation and temperatures.

The analysis of temperatures showed a clear – and expected – dependence on elevation except for tropical nights, when the Mediterranean side reached values higher than 30 days per year and in the rest of the mountain range was anecdotal. General significant positive trends were observed at annual and seasonal scales since mid-twentieth century (1959) ranging from 0.17 °C/decade in winter to 0.43 °C/decade in summer. The highest values of these trends were reached by maximum temperatures in all seasons and in summer in mean and minimum temperatures.

The precipitation indices, particularly those concerning the number of rainy days (like CDD, CWD, R95rel), revealed a distinct latitudinal pattern. This pattern illustrates the wetter conditions on the northern slope of the Pyrenees and the more irregular precipitation patterns in the southern regions. Other indices related to precipitation magnitude (RX1, RX5, R10mm, R20mm) showed a longitudinal spatial pattern with higher frequency of precipitation extremes in Atlantic side than the Mediterranean one. The only significant trends for the 1959–2020 period were found at annual scale on southern and Mediterranean sides of the Pyrenees, showing a decrease at a rate near to 3 % per decade. Seasonal trends did not reflect significant changes.

All of these contributions to the knowledge of the climate of the Pyrenees are based on several novelties regarding previous works: 1) the joint use of climatic observations from both sides of the mountain range facilitated the complete climatic analysis, 2) the use of the same reconstruction method made the results comparable between sides; and 3) the provision of essential climatic variables through a gridded dataset at an unprecedented spatial resolution and through long-term homogenized data series showed, for the first time, an integrated trend analysis for the whole mountain range and the spatial and temporal patterns of extreme climate indices not seen before as a whole in the Pyrenees.

The new daily gridded dataset, which is publicly available, is an opportunity to develop multiple potential applications related to recognition and mitigation of climate-related events directly affecting the environment and related socio-economic activities. It is continuously updated with new data, recent periods and, potentially, higher resolution. In addition, the recent concession of the LIFE22-IPC-ES LIFE-PYRENEES4CLIMA (2023−2031) will deepen the knowledge of variability and climate change observed in the Pyrenees, providing new databases, with the incorporation of new variables and higher temporal coverage and resolutions.

Funding

This study was funded by the project CLIMPY: "Characterization of the evolution of climate and provision of information for adaptation in the Pyrenees" (EFA081/15 Interreg V-A POCTEFA 2014-2020); and OPCC-ADAPYR: "Capitalization, observation, transfer and appropriation of adaptation strategies to climate change in the Pyrenees" (EFA346/19 Interreg V-A POCTEFA 2014-2020). RSN is supported by grant RYC2021-034330-I funded by MCIN/AEI/10.13039/501100011033 and by "European Union NextGenerationEU/PRTR". ET is funded by a Marie Skłodowska-Curie Action (ITHACA-101024389).

CRediT authorship contribution statement

José María Cuadrat: Writing – original draft, Resources, Funding acquisition, Conceptualization. **Roberto Serrano-Notivoli:** Writing – review & editing, Writing – original draft, Visualization, Validation, Software, Methodology, Formal analysis. **Marc Prohom:** Writing – review & editing, Writing – original draft, Methodology, Formal analysis.

Jordi Cunillera: Writing – review & editing, Writing – original draft, Methodology, Formal analysis. **Ernesto Tejedor:** Writing – review & editing, Visualization, Formal analysis. **Miguel Ángel Saz:** Writing – review & editing, Conceptualization. **Martín de Luis:** Writing – review & editing, Validation, Software, Methodology, Formal analysis. **Alba Llabrés-Brustenga:** Writing – review & editing, Methodology, Formal analysis. **Jean-Michel Soubeyroux:** Resources, Funding acquisition, Formal analysis.

Declaration of competing interest

The authors declare that they have no known competing financial interests or personal relationships that could have appeared to influence the work reported in this paper.

Data availability

Data can be accessed from: https://zenodo.org/doi/10.5281/zenodo.3611126

Acknowledgements

Authors thank to weather station networks managers in the Pyrenees for providing data (Agencia Estatal de Meteorología, Euskalmet, MétéoFrance, Servei Meteorològic de Catalunya and Servei Meteorològic Nacional d'Andorra).

Appendix A. Supplementary data

Supplementary data to this article can be found online at https://doi.org/10.1016/j.scitotenv.2024.173052.

References

Aguilar, E., Auer, I., Brunet, M., Peterson, T.C., Wieringa, J., 2003. Guidelines on Climate Metadata and Homogenization; WCDMP-53, WMO-TD 1186. World Meteorological Organization, Geneva, Switzerland.

Albalat, A., Trapero, L., Lemus, M., Pons, M., 2022. Indicadores para el análisis de la evolución del espesor del manto de nieve en las estaciones de esquí: el caso de Andorra. In: XII Congreso Internacional de la Asociación Española de Climatología, pp. 655–665.

Auer, I., Böhm, R., Jurkovic, A., Lipa, W., Orlik, A., Potzmann, R., Schöner, W., Ungersböck, M., Matulla, C.H., Briffa, K., Jones, P., Efthymiadis, D., Brunetti, M., Nanni, T., Maugeri, M., Mercalli, L., Mestre, O., Moisselin, J.M., Begert, M., Müller-Westermeier, G., Kveton, V., Bochnicek, O., Stastny, P., Lapin, M., Szalai, S., Szentimrey, T., Cegnar, T., Dolinar, M., Gajic-Capka, M., Zaninovic, K., Majstorovicp, Nieplovaq, E., 2007. HISTALP — historical instrumental climatological. Surface time series of the Greater Alpine Region. Int. J. Climatol. 27, 17–46. https://doi.org/10.1002/joc.1377.

Beniston, M., Diaz, H.F., Bradley, R.S., 1997. Climatic change at high elevation sites: an overview. Clim. Change 36, 233–251. https://doi.org/10.1023/A:1005380714349.

Bonsoms, J., González, S., Prohom, M., Esteban, P., Salvador-Franch, F., López-Moreno, J.I., Oliva, M., 2021. Spatio-temporal patterns of snow in the Catalan Pyrenees (NE Iberia). Int. J. Climatol. 41 (12), 5676–5697. https://doi.org/10.1002/joc.7147.

Bücher, A., Dessens, J., 1991. Secular trend of surface temperature at an elevated observatory in the Pyrenees. J. Climate 4, 859–868.

Buisán, S., Saz, M.A., López-Moreno, J.I., 2015. Spatial and temporal variability of winter snow and precipitation days in the western and central Spanish Pyrenees. Int. J. Climatol. 35, 259–274. https://doi.org/10.1002/joc.3978.

Buisán, S., López-Moreno, J.I., Saz, M.A., Kochendorfer, J., 2016. Impact of weather type variability on winter precipitation, temperature and annual snowpack in the Spanish Pyrenees. Climate Res. 69, 79–92. https://doi.org/10.3354/cr01391.

CARPATCLIM, 2013. Deliverable 3.7. http://www.carpatclim-eu.org/docs/deliverables/D3_7.pdf.

Cheval, S., Birsan, M.V., Dumitrescu, A., 2014. Climate variability in the Carpathian Mountains Region over 1961–2010. Global Planet. Change 118, 85–96. https://doi.org/10.1016/j.gloplacha.2014.04.005.

Cuadrat, J.M., Saz, M.A., Vicente-Serrano, S., 2007. Atlas climático de Aragón. Gobierno de Aragón, Zaragoza, 222 p. ISBN 978-84-8380-071-3.

Daly, C., Slater, M.E., Roberti, J.A., Laseter, S.H., Swift, L.W., 2017. High-resolution precipitation mapping in a mountainous watershed: ground truth for evaluating uncertainty in a national precipitation dataset. Int. J. Climatol. 37 (S1), 124–137. https://doi.org/10.1002/joc.4986.

Deaux, A., Soubeyroux, J.M., Cuadrat, J.M., Cunillera, J., Prohom, M., 2014. Homogénéisation transfrontalière des températures sur le massif des Pyrénées. Rev. Climatol. 24, 67–78.

Domonkos, P., 2022. ACMANTv4: scientific content and operation of the software, 71p. Available online: https://github.com/dpeterfree/ACMANT. accessed on 24 November 2023.

Domonkos, P., Guijarro, J.A., Venema, V., Brunet, M., Sigró, J., 2021. Efficiency of time series homogenization: method com-parison with 12 monthly temperature test datasets. J. Climate 34, 2877–2891. https://doi.org/10.1175/JCLI-D-20-0611.1.

El Kenawy, A., López-Moreno, J.I., Vicente-Serrano, S.M., 2011. Recent trends in daily temperature extremes over northeastern Spain (1960–2006). Nat. Hazards Earth Syst. Sci. 11, 2583–2603. https://doi.org/10.5194/nhess-11-2583-2011.

El Kenawy, A., López-Moreno, J.I., Vicente-Serrano, S.M., 2013. Summer temperature extremes in northeastern Spain: spatial regionalization and links to atmospheric circulation (1960–2006). Theor. Appl. Climatol. 113, 387–405. https://doi.org/10.1007/s00704-012-0797-5.

Espejo, F., Ferraz, J., Palomo, M., 2008. Tendencias recientes en las series de temperatura del Pirineo Central y Occidental. Asoc. Esp. Climatol. 6, 99–108.

Esteban, P., Prohom, M., Aguilar, E., 2012. Tendencias recientes e índices de cambio climático de la temperatura y la precipitación en Andorra, Pirineos (1935–2008). Pirineos 167, 87–106. https://doi.org/10.3989/Pirineos.2012.167005.

Gascoin, S., Hagolle, O., Huc, M., Jarlan, L., Dejoux, J.-F., Szczypta, C., Marti, R., Sánchez, R., 2015. A snow cover climatology for the Pyrenees from MODIS snow products. Hydrol. Earth Syst. Sci. 19, 2337–2351. https://doi.org/10.5194/hess-19-2337-2015.

Giorgi, F., Hurrell, J.W., Marinucci, M.R., Beniston, M., 1997. Elevation dependency of the surface climate change signal: a model study. J. Climate 10, 288–296.

Guijarro, J.A., López, J.A., Aguilar, E., Domonkos, P., Venema, V., Sigró, J., Brunet, M., 2017. Comparison of homogenization packages applied to monthly series of temperature and precipitation: the MULTITEST project. In: Ninth Seminar for Homogenization and Quality Control in Climatological Databases. WMO.WCDMP-85, Geneva, pp. 46–62.

Hofstra, N., Haylock, M., New, M., Jones, P., Frei, C., 2008. Comparison of six methods for the interpolation of daily, European climate data. J. Geophys. Res. 113, D21110. https://doi.org/10.1029/2008JD010100.

Hofstra, N., New, M., McSweenwy, C., 2010. The influence of interpolation and station network density on the distributions and trends of climate variables in gridded daily data. Climate Dynam. 35, 841–858. https://doi.org/10.1007/s00382-009-0698-1.

IPCC, 2021. In: Masson-Delmotte, et al. (Eds.), Climate Change 2021: The Physical Science Basis. Contribution of Working Group I to the Sixth Assessment Report of the Intergovernmental Panel on Climate Change. Cambridge University Press, Cambridge and New York. https://doi.org/10.1017/9781009157896.001.

Isotta, F.A., Frei, C., Weilguni, V., Perčec Tadic, M., Lassègues, P., Rudolf, B., Pavan, V., Cacciamani, C., Antolini, G., Ratto, S.M., Munari, M., Micheletti, S., Bonati, V., Lussana, C., Ronchi, C., Panettieri, E., Marigo, G., Vertačnik, G., 2014. The climate of daily precipitation in the Alps: development and analysis of a high-resolution grid dataset from pan-Alpine rain-gauge data. Int. J. Climatol. 34, 1657–1675. https://doi.org/10.1002/joc.3794.

JCR, 2010. Climate of the Carpathian Region. European Commission Join Research Centre. http://desert.jcr.ec.europa.eu/action/php/index.php.

Kendall, M.G., 1975. Rank Correlation Methods, 4th edition. Charles Griffin, London.

Klein Tank, A., Zwiers, F., Zhang, X., 2009. Guidelines on analysis of extremes in a changing climate in support of informed decisions for adaptation. In: World Meteorological Organization, Report WCDMP-No.72, WMO-TD 1500, Geneva, Switzerland, 52 pp. http://www.clivar.org/organization/etccdi/etccdi.php.

Lana, F., Burgueño, A., Martínez, M.D., Serra, C., 2009. Una revisión de los análisis estadísticos de las precipitaciones diarias y mensuales en Catalunya. Tethys 6, 15–30. https://doi.org/10.3369/tethys.2009.6.02.

Lemus-Canovas, M., López-Bustins, J.A., 2021. Assessing internal changes in the future structure of dry-hot compound events: the case of the Pyrenees. Nat. Hazards Earth Syst. Sci. 21, 1721–1738. https://doi.org/10.5194/nhess-21-1721-2021.

Lemus-Canovas, M., Lopez-Bustins, J.A., Trapero, L., Martin-Vide, J., 2019. Combining circulation weather types and daily precipitation modelling to derive climatic precipitation regions in the Pyrenees. Atmos. Res. 220, 181–193. https://doi.org/10.1016/j.atmosres.2019.01.018.

Lemus-Canovas, M., Lopez-Bustins, J.A., Martín-Vide, J., Halifa-Marin, A., Insua-Costa, D., Martinez-Artigas, J., Trapero, L., Serrano-Notivoli, R., Cuadrat, J.M., 2021. Characterisation of extreme precipitation events in the Pyrenees: from the local to the synoptic scale. Atmosphere 12 (6), 665. https://doi.org/10.3390/atmos12060665.

López-Moreno, J.I., Goyette, S., Beniston, M., 2008. Climate change prediction over complex areas: spatial variability of uncertainties and prediction over the Pyrenees from a set of regional climate models. Int. J. Climatol. 28 (11), 1535–1550. https://doi.org/10.1002/joc.1645.

López-Moreno, J.I., Vicente-Serrano, S.M., Angulo-Martínez, M., Beguería, S., Kenawy, A., 2010. Trends in daily precipitation on the northeastern Iberian Peninsula, 1955–2006. Int. J. Climatol. 30, 1026–1041. https://doi.org/10.1002/joc.1945.

López-Moreno, J.I., Soubeyroux, J.-M., Gascoin, S., Alonso-Gonzalez, E., Durán-Gómez, N., Lafaysse, M., Vernay, M., Carmagnola, C., Morin, S., 2020. Long-term trends (1958–2017) in snow cover duration and depth in the Pyrenees. Int. J. Climatol. 40 (14), 6122–6136. https://doi.org/10.1002/joc.6571.

Mann, H.B., 1945. Nonparametric tests against trend. Econometrica 13, 245–259.

Maris, M., Giraud, G., Durand, Y., Navarre, J.P., Mérindol, L., 2009. Results of 50 years of climate reanalyses in the French Pyrenees (1958–2008) using the SAFRAN and CROCUS models. In: Davos: International Snow Science Workshop, Proceedings.

Martin-Vide, J., 2004. Spatial distribution of a daily precipitation concentration index in peninsular Spain. Int. J. Climatol. 24 (8), 959–971. https://doi.org/10.1002/joc.1030.

Merino, A., García-Ortega, E., Navarro, A., Fernandez-Gonzalez, S., Tapiador, F.J., Sanchez, J.L., 2021. Evaluation of gridded rain-gauge-based precipitation datasets: impact of station density, spatial resolution, altitude gradient and climate. Int. J. Climatol. 41, 3027–3043. https://doi.org/10.1002/joc.7003.

Navarro-Serrano, F., López-Moreno, J.I., Azorin-Molina, C., Alonso-Gonzalez, E., Tomas-Burguera, M., Sanmiguel-Vallelado, A., Revuelto, J., Vicente-Serrano, S.M., 2018. Estimation of near-surface air temperature lapse rates over continental Spain and its mountain areas. Int. J. Climatol. 38, 3233–3249. https://doi.org/10.1002/joc.5497.

Nigrelli, G., Chiarle, M., 2023. 1991–2020 climate normal in the European Alps: focus on high-elevation environments. J. Mt. Sci. 20 (8) https://doi.org/10.1007/s11629-023-7951-7.

OPCC-CTP, 2018. El cambio climático en los Pirineos: impactos, vulnerabilidades y adaptación. In: Bases de conocimiento para la futura estrategia de adaptación al cambio climático en los Pirineos. Observatorio Pirenaico del Cambio Climático, 150 p. ISBN: 978-84-09-06268-3.

Pepin, N.C., Lundquist, J.D., 2008. Temperature trends at high elevations: patterns across the globe. Geophys. Res. Lett. 35 (14), L14701. https://doi.org/10.1029/2008GL034026.

Pérez-Zanón, N., Sigró, J., Ashcroft, L., 2017. Temperature and precipitation regional climate series over the central Pyrenees during 1910–2013. Int. J. Climatol. 37, 1922–1937. https://doi.org/10.1002/joc.4823.

Rubel, F., Brugger, K., Haslinger, K., Auer, I., 2017. The climate of the European Alps: shift of very high resolution Köppen-Geiger climate zones 1800–2100. Meteorol. Z. 26, 115–125. https://doi.org/10.1127/metz/2016/0816.

Serrano-Notivoli, R., de Luis, M., Saz, M.A., Beguería, S., 2017a. Spatially based reconstruction of daily precipitation instrumental data series. Climate Res. 73, 167–186. https://doi.org/10.3354/cr01476.

Serrano-Notivoli, R., Beguería, S., Saz, M.A., De Longares, L.A., Luis, M., 2017b. SPREAD: a high-resolution daily gridded precipitation dataset for Spain—an extreme events frequency and intensity overview. Earth Syst. Sci. Data 9 (2), 721–738. https://doi.org/10.5194/essd-9-721-2017.

Serrano-Notivoli, R., Buisán, S., Abad, L.M., Sierra, E., López-Moreno, J.I., Cuadrat, J.M., 2018. Tendencias recientes en precipitación, temperatura y nieve de alta montaña en los Pirineos. In: Montávez, J.P., et al. (Eds.), El clima: aire, agua, tierra y fuego, vol. 11. Asociación Española de Climatología, pp. 267–280. ISBN: 978-84-7837-098-6.

Serrano-Notivoli, R., Beguería, S., De Luis, M., 2019. STEAD: a high-resolution daily gridded temperature dataset for Spain. Earth Syst. Sci. Data 11, 1171–1188. https://doi.org/10.5194/essd-11-1171-2019.

Soubeyroux, J.M., Jourdain, S., Grimal, D., Espejo, F., Esteban, P., Merz, T., 2011. Approche transfrontalière pour l'inventaire et la valorisation des données climatologiques sur le Massif des Pyrénées. In: Colloque SHF «Eaux en montagne». Lyon, pp. 344–350.

Spagnoli, B., Planton, S., Mestre, O., Déqué, M., Moisselin, J.M., 2002. Detecting climate change at a regional scale: the case of France. Geophys. Res. Lett. 29 (10), 91–94.

Squintu, A.A., van der Schrier, G., Stepanek, P., Zahararnichek, P., Tank, A.K., 2020. Comparison of homogenization methods for daily temperature series against an observation-based benchmark dataset. Theor. Appl. Climatol. 140 (1-2), 285–301. https://doi.org/10.1007/s00704-019-03018-0.

Venema, V., Mestre, O., Aguilar, E., Auer, I., Guijarro, J.A., Domonkos, P., Vertacnik, G., Szentimrey, T., Stepanek, P., Zahradnicek, P., Viarre, J., Müller-Westermeier, G., Lakatos, M., Williams, C.N., Menne, M.J., Lindau, R., Rasol, D., Rustemeier, E., Kolokythas, E., Marinova, T., Andresen, L., Acquaotta, F., Fratianni, S., Cheval, S., Klancar, M., Brunetti, M., Gruber, C., Prohom, M., Likso, T., Esteban, P., Brandsma, T., 2012. Benchmarking monthly homogenization algorithms. Clim. Past 8, 89–115. https://doi.org/10.5194/cp-8-89-2012.

Venema, V., Trewin, B., Wang, X.L., Szentimrey, T., Lakatos, M., Aguilar, E., Auer, I., Guijarro, J., Menne, M., Oria, C., et al., 2020. Guidelines on Homogenization. World Meteorological Organization, Geneva, p. 1245.

Wang, Q., Fan, X., Wang, M., 2014. Recent warming amplification over high elevation regions across the globe. Climate Dynam. 43, 87–101. https://doi.org/10.1007/s00382-013-1889-3.

Williams, M., Eggieston, S., 2017. Using indicators to explain our changing climate to policymakers and the public. Bull. WMO 66 (2), 201.